NANOSYSTEMS:
PHYSICS, CHEMISTRY, MATHEMATICS

Original article

Korableva G.M., et al. *Nanosystems: Phys. Chem. Math.*, 2025, **16** (4), 0–6.
http://nanojournal.ifmo.ru
DOI 10.17586/2220-8054-2025-16-4-0-6

Pt/CeO_2–ZrO_2 catalyst for dimethyl ether and dimethoxymethane partial oxidation to syngas: in-situ Raman spectroscopy structural studies

Galina M. Korableva[1,a], Dmitrii A. Agarkov[1,2,b], Sukhe D. Badmaev[3,c], Denis S. Katrich[1,d], Alexandr V. Samoilov[1,e], Pavel V. Snytnikov[3,f], Ilya I. Tartakovskii[1,g], Sergey I. Bredikhin[1,h]

[1]Osipyan Institute of Solid State Physics RAS, Chernogolovka, Moscow District, Russia
[2]Moscow Institute of Physics and Technology, Dolgoprudny, Moscow District, Russia
[3]Boreskov Institute of Catalysis SB RAS, Novosibirsk, Russia

[a]eliseevagm@issp.ac.ru, [b]agarkov@issp.ac.ru, [c]sukhe@catalysis.ru, [d]katrich.ds@phystech.edu, [e]samoilov@issp.ac.ru, [f]pvsnyt@catalysis.ru, [g]tartakov@issp.ac.ru, [h]bredikh@issp.ac.ru

Corresponding author: Dmitrii A. Agarkov, agarkov@issp.ac.ru

PACS 88.30.M-, 82.45.Jn, 81.16.Hc, 82.80.Gk

ABSTRACT This paper is devoted to studies of the conversion mechanism of carbon-containing fuels on multicomponent catalyst with the composition of 1.9 wt. % Pt–$Ce_{0.75}Zr_{0.25}O_2$ (Pt/CZ) using in-situ Raman spectroscopy (RS) and catalytic activity measurements. It was found that during heating and transition from inert atmosphere to reducing conditions, oxygen escapes from the crystal lattice of the samples. This leads to formation of oxygen vacancies in the near-surface layer of the catalyst and increasing Ce^{3+} concentration by more than 20 % already at a temperature of 400 °C. Meanwhile, when returning to the initial external conditions (temperature, gas mixture), a reversible process occurs. The use of Pt/CZ catalysts allows to obtain up to 35 vol % H_2 and about 25 vol % CO in syngas during dimethyl ether and dimethoxymethane partial oxidation. Thus, Pt/CZ catalysts are of particular interest as efficient catalysts for the conversion of hydrocarbons to synthesis gas, suitable for feeding SOFC stacks.

KEYWORDS partial oxidation, dimethyl ether, dimethoxymethane, Raman spectroscopy, Pt/CeO_2–ZrO_2, catalyst

FOR CITATION Korableva G.M., Agarkov D.A., Badmaev S.D., Katrich D.S., Samoilov A.V., Snytnikov P.V., Tartakovskii I.I., Bredikhin S.I. Pt/CeO_2–ZrO_2 catalyst for dimethyl ether and dimethoxymethane partial oxidation to syngas: in-situ Raman spectroscopy structural studies. *Nanosystems: Phys. Chem. Math.*, 2025, **16** (4), 0–6.

1. Introduction

Power plants based on solid oxide fuel cells (SOFC) are promising power sources due to their record high efficiency and high power density, as well as they are capable to use different hydrocarbons as a fuel [1, 2]. SOFC stacks give opportunity to operate being fed by not only hydrogen, but also syngas (H_2+CO) [3, 4]. The most promising way of SOFC development is the transition to the use of various hydrocarbon fuels (methane, propane, natural gas and others). Besides, to maintain the high electrochemical efficiency of SOFC, it is necessary to convert hydrocarbon fuels in an external fuel processor. It is also necessary to convert hydrocarbon fuels to obtain a high quantity of hydrogen and CO in the resulting fuel mixture. Thus, the development of highly efficient catalysts for the conversion of hydrocarbons to syngas is an extremely important task.

Dimethoxymethane (DMM) and dimethyl ether (DME) are environmentally benign oxygenated compounds of C1 chemistry with a wide scope of applications. Nowadays, these compounds are generally produced from methanol. DME and DMM synthesis using renewable feedstocks, namely, CO_2 produced from biomass and hydrogen generated by water electrolysis is under development now. In past decades, DMM and DME have been recognized as a promising feedstock for hydrogen production for fuel cell feeding [5, 6]. Recently, we proposed efficient catalyst Pt/CZ for DME and DMM partial oxidation (PO) to syngas [5] showing high promises for SOFC applications. The reason for this catalyst choice is that noble metal-based catalysts are known for their high performance in PO of methanol [7] and PO of DME [8]. It is well known that CeO_2–ZrO_2 solid solution is a good support for noble metals [8, 9]. Catalytic activity of such catalysts is associated with surface oxygen vacancy formation [10–12].

This paper presents the results of the study of Pt/CZ catalyst for PO of DMM and DME. The aim of this work was to investigate this catalyst by means of in-situ Raman spectroscopy as a supplement to standard catalysis techniques.

2. Experimental section

2.1. Catalyst samples preparation

$Ce_{0.75}Zr_{0.25}O_2$ (CZ) produced by Ecoalliance LLC (Russia) was used as the support material. The CZ support had a fluorite structure with a size of coherent scattering region of $\sim$ 11 nm and a specific surface area of $\sim$ 70 m^2/g. Pt-supported on CZ (Pt/CZ) catalyst was prepared by sorption-hydrolytic deposition [5, 6]. This method is based on kinetic inertness of metal complexes to hydrolysis at a room temperature and the main idea of this method is to obtain a solution of "noble metal salt + alkaline agent", which is metastable under given conditions (temperature, concentration) with respect to the precipitation of homogeneous metal hydroxide. Since the support surface accelerates the heterogeneous nucleation and growth of metal hydroxide particles, the addition of the support particles to the reagent mixture initiates hydrolysis, resulting in uniform deposition of metals on the particles' surface. The preparation of the Pt/CZ catalyst began with a $K_2[PtCl_4]$ salt been dissolved in water and CZ powder been added to the solution. Then, while stirring, a solution of Na_2CO_3 ($K_2[PtCl_4]$: Na_2CO_3 = 1 : 1.1 mol:mol) was added drop by drop, after which it was left to stir at 20 °C for 10 minutes, then at 80 °C for 30 minutes. After this the solution was checked using $NaBH_4$ for the presence of platinum ions, which were not detected. Next, the powder was separated from the solution, washed and kept in a furnace at 80 °C for 7 hours. Then the powder was calcined in a stream of Ar at 100 °C for 10 minutes, then in a stream of H_2 for 10 minutes at 100, 200 and 300 °C and for 30 minutes at 350 °C.

The resulting powder of the composition 1.9 wt. % Pt/$Ce_{0.75}Zr_{0.25}O_2$ with bulk density about 1 g/cm^3 was pressed into a pellet weighing 0.25 g and 20 mm in diameter. For RS studies samples of 4×4 mm were laser-cut from the pellet.

2.2. Experimental techniques

Catalyst structure was accessed using X-ray diffraction (XRD, Rigaku SmartLab SE, CuKα λ = 1.54178 Å radiation, 40 kV, 35 mA, 2θ = 20 – 100 °).

RS studies were performed by means of home-made combined in-situ technique described previously [13, 14]. A laser with a wavelength of 532 nm is used as a source of exciting radiation. The system gives opportunity to carry out experiments under various operating conditions: from room temperature to 1000 °C, in gas flows of H_2, CH_4, CO/CO_2, N_2, O_2 up to 100 ml/min. The sequence of spectroscopic measurements is presented in Table 1: acquisition of each spectrum began after stabilization in mentioned conditions for 20 minutes. Samples were studied in an inert and a reaction mixture atmosphere at 400 and 700 °C. The temperatures were chosen according to experimental results: Pt/CZ catalyst exhibit high efficiency of partial oxidation of DME and DMM at these temperatures (see Section 3).

TABLE 1. Sequence and conditions of spectroscopic measurements

Step	Temperature,°C	Gas
#1	400	Inert: 200 ml/min N_2
#2	700	Inert
#3	400	Inert
#4	400	Fuel: 180 ml/min N_2+10 ml/min H_2+10 ml/min CO
#5	700	Fuel
#6	400	Fuel

Thermogravimetric (TG) analysis was carried out using TG 209 F1 Iris thermobalance (NETZSCH). These measurements used atmosphere of 5 % H_2 in Ar as model reducing gas (total flow 70 ml/min), heating was at a rate of 10 K/min from 25 to 600 °C.

The DME and DMM PO reactions were performed under ambient pressure in temperature range of 300 – 700 °C in a fixed-bed quartz continuous flow reactor (6 mm i.d.) with two inlets for separate supply of oxygen and DMM/DME to prevent homogeneous oxidation in the gas phase [5, 6]. The gas streams were mixed immediately before the catalyst bed. Reaction mixture composition for these experiments was 28.6 vol % DMM or DME, 14.3 vol % O_2, 57.1 vol % N_2 (fuel:air = 5:2) and GHSV = 10000 h^{-1}. The catalyst temperature was measured by a chromel/alumel thermocouple positioned in the center of the catalyst bed. The compositions of the inlet and outlet gas mixtures were evaluated by a gas chromatograph (GC Chromos-1000) equipped with two thermal conductivity detectors (TCD).

The analysis of the surface composition and compositional homogeneity of the supported particles was performed using a high-angle annular dark field scanning transmission electron microscopy (HAADFSTEM) images and energy-dispersive X-ray (EDX) patterns. The experiments were performed using an electron microscope JEm2200FS ("JEOL", Japan) equipped with a HAADF detector to obtain images of high atomic contrast in scanning mode and with EDX-analyzer for local microanalysis and EDX-local mapping.

3. Results and discussion

The Pt/CZ catalyst before and after in-situ RS studies were characterized by XRD (Fig. 1 top and bottom, Table 2). All samples have a fluorite-type structure (space group $Fm\bar{3}m$) with cell parameters 5.400 and 5.394 Å before and after measurements. Calculation of the crystalline sizes using Scherrer's equation yielded average sizes of 11.5 and 11.3 nm for the catalyst before and after testing, respectively. Thus, negligible change in cell parameters and crystalline size supports the idea that experiment does not affect the catalyst's structure.

No peaks related to metallic phases were observed due to the low concentration or well dispersed Pt species.

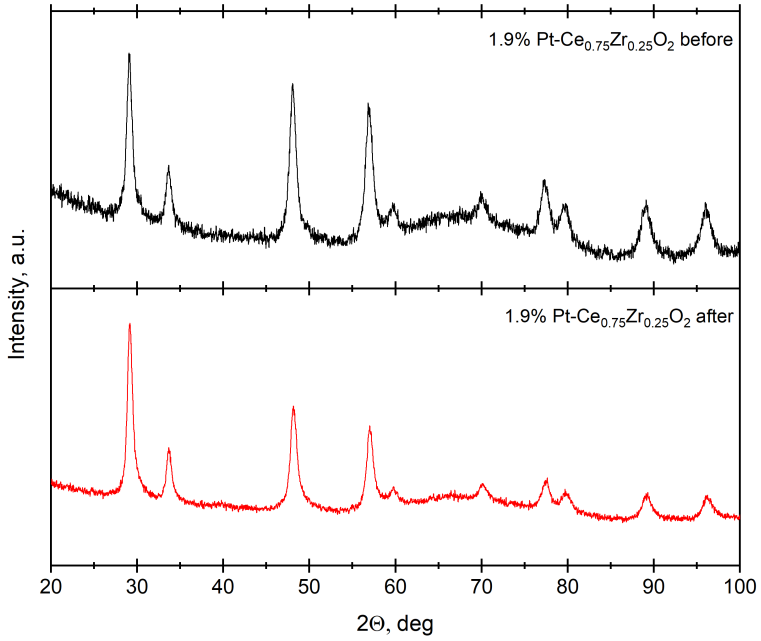

FIG. 1. XRD patterns of Pt/CZ before (top) and after (bottom) the measurements

TABLE 2. The parameters of the unit cell of the samples and particle sizes obtained from the XRD data

Before/after measurements	Phase composition	a, Å	V, Å^3	Particle size, nm
before	Cubic $Fm\bar{3}m$ (225)	5.400	157.4	11.5
after	Cubic $Fm\bar{3}m$ (225)	5.394	156.9	11.3

Figure 2 illustrates the effect of temperature on the DMM/DME conversions and the outlet H_2 and CO concentrations in PO of DMM (a) and DME (b) over Pt/CZ catalyst. The respective thermodynamic equilibrium values of conversions, H_2 and CO concentrations are also shown for comparison. One can see that DME and DMM conversions increase with temperature and reach $\sim$ 100 % at 400°C. However, the effect of the temperature on the H_2 and CO concentrations in reactions of PO of DME/DMM follow wavy curve. In PO of DMM (Fig. 2a), two temperature regions were observed at which the H_2+CO sum concentrations exceeded 50 vol. %. For low-temperature region ($\sim$ 400 °C) kinetic control is responsible for H_2 and CO production whereas at high-temperature region the concentrations are close to the equilibrium ones. It means that the Pt/CZ catalyst is efficient in terms of producing syngas at a low temperature. The data obtained in Fig. 2 demonstrate that the Pt/CZ catalyst provides syngas production with nearly the same H_2 (and CO) content both at temperatures of 400 and 700 °C in PO of DMM. Most likely that the low-temperature products formation is governed by the progress of elementary stages suggested in works [5, 6]. These stages proceed with involvement of oxygen from the surface of Pt nanoparticles (Pt–O) while oxygen transport from crystal lattice of the CeO_2–ZrO_2 catalyst support plays a main role in the formation of such surface bonds.

For both DMM and DME partial oxidation reactions at 700 °C the H_2 and CO concentrations are close to 35 and 25 vol. % respectively, whereas the conversion rates of DMM and DME are close to 100 % at 700 °C.

According to the data above main temperatures of 400 and 700 °C were chosen to perform spectroscopic Raman measurements. Fig. 3a shows the "initial" Raman spectra which were obtained in inert atmosphere at a room temperature (lower curve) and 400 °C (middle curve) and in mixture N_2:H_2:CO = 90:5:5 at 400 °C (upper curve). The most intense line (457 cm^{-1}) belongs to F_{2g} symmetric vibration mode in ceria [15, 16]. The spectra reveal lines responsible for vibrations

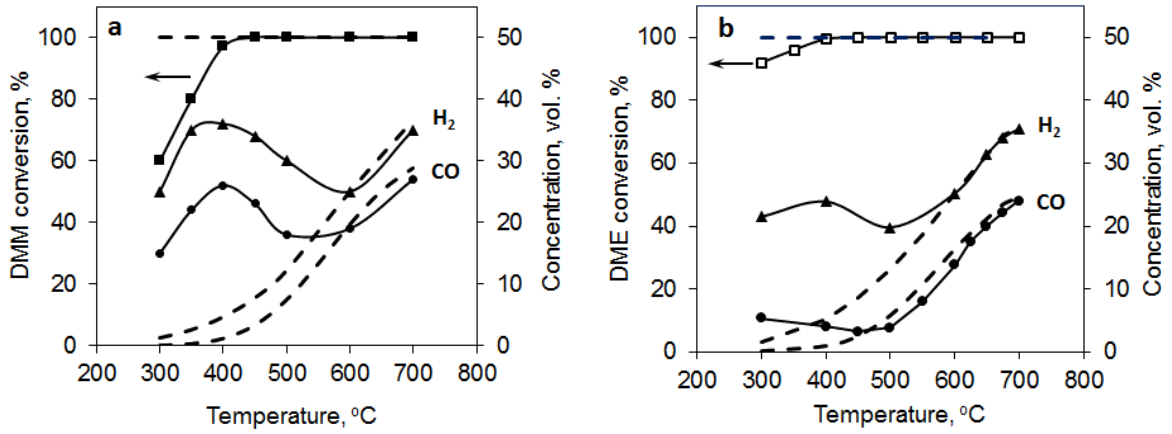

FIG. 2. Effect of temperature on DMM and DME conversions and H_2 and CO concentrations in DMM (a) and DME (b) partial oxidation over the Pt/CeO_2–ZrO_2 catalyst. Solid lines – experiment, dotted – thermodynamic equilibrium values

of bound oxygen on platinum: ~ 690 cm^{-1} for Pt–O–Ce vibrations [17] and ~ 665 cm^{-1} refers to Pt–O_x vibrations [18]. However, the bond of platinum with oxygen is weakly detected by RS due to low concentration (1.9 wt. %) of platinum and it's distribution over the catalyst surface in form of nanoparticles. Also there are "parasitic" peaks in the spectrum characterizing vibrations in Al2O3 (380, 420 and 630 cm^{-1}) [19], which appear due to presence of "viewing window" made of artificial sapphire.

Heating the Pt/CZ catalyst in an inert atmosphere leads to changes in the spectra. Firstly, the mode of symmetric F_{2g} vibrations in CeO_2 undergoes changes: the intensity decreases, and the line broadens. These facts indicate the release of oxygen from the crystal lattice of the catalyst and the formation of vacancies upon heating. Secondly, the lines characterizing the vibrations of the Pt–O_x bond disappear. These bonds are formed on the surface of the catalyst with platinum nanoparticles and are highly sensitive to the presence of oxygen. According to the literature [20], while heating the catalyst the bonds with surface oxygen are broken first (Pt–O), then bonds with intranodal oxygen (Pt–O–Ce). The temperature at which these vibration lines become undetectable is ~ 200 °C.

Figure 3b shows the spectra of the catalyst collected in accordance with the measurement sequence (Table 1). Main changes occur in the line of symmetrical vibrations of ceria (~ 440 cm^{-1}). For a more detailed study this peak was separated from the spectrum, results are shown in Fig. 3c. Considering intensity of this peak at step #1 as 100 %, we can state that at step #3 the intensity has dropped down by 18 %, while transition to reducing atmosphere (step #4) decreased this intensity to more than 40 % of the initial value. In this context intensity decrease of the line of symmetrical vibrations of ceria indicates an increase in the proportion of cerium Ce^{3+} by the corresponding value.

The dependencies of the position and half-width of this line on the program step are shown in Fig. 3d. A strong (up to 10 cm^{-1}) shift of the oscillation band to the short-wavelength region occurs during heating (steps #2 and #5). It can be explained by the softening of the vibrational mode due to an increase in temperature, and secondly, to the release of oxygen from the crystal lattice and the transition $Ce^{4+} \rightarrow Ce^{3+}$. The dependence of the peak half-width on temperature confirms this idea: upon heating, the line undergoes a strong broadening associated with the formation of defects [15, 21]. Moreover, a shift of the oscillation band to the short-wavelength region is also observed upon transition from inert to reducing atmosphere (a gas mixture with the addition of 5 % CO and 5 % H_2). This fact is related to the reduction of the catalyst and the transition $Ce^{4+} \rightarrow Ce^{3+}$. After cooling (steps #2→#3 and #5→#6) both the peak position and the line half-width return to their origin (before heating by 700 °C) which indicates the possibility of thermal cycling of these catalysts during their operation without changing their crystalline properties. This "re-oxidation" occurred because of inevitable small air leaks into the reaction chamber.

The catalyst support (CZ) was studied by thermogravimetric analysis (Fig. 4). One can see a systematic loss of mass while heating the catalyst support in a reducing atmosphere. The total mass loss was less than 3 % at the end of the measurement (at 600 °C) which corresponds to the release of oxygen from the crystal lattice. Thus, the TG data strongly support the results obtained using Raman spectroscopy.

The analysis of the surface composition and compositional homogeneity of supported particles in Pt/CZ catalyst was performed using a HAADF-STEM technique (Fig. 5a) with EDX mapping analysis (b–d). Fig. 5a shows the morphology of the catalyst: particles with a characteristic size of ~ 10 – 20 nm with spots of ~ 2 nm on their surface. Using element mapping (Fig. 5b–d) we conclude that Pt particles (~ 2 nm) are uniformly distributed over the surface of CZ support particles, which are 10 – 20 nm in size.

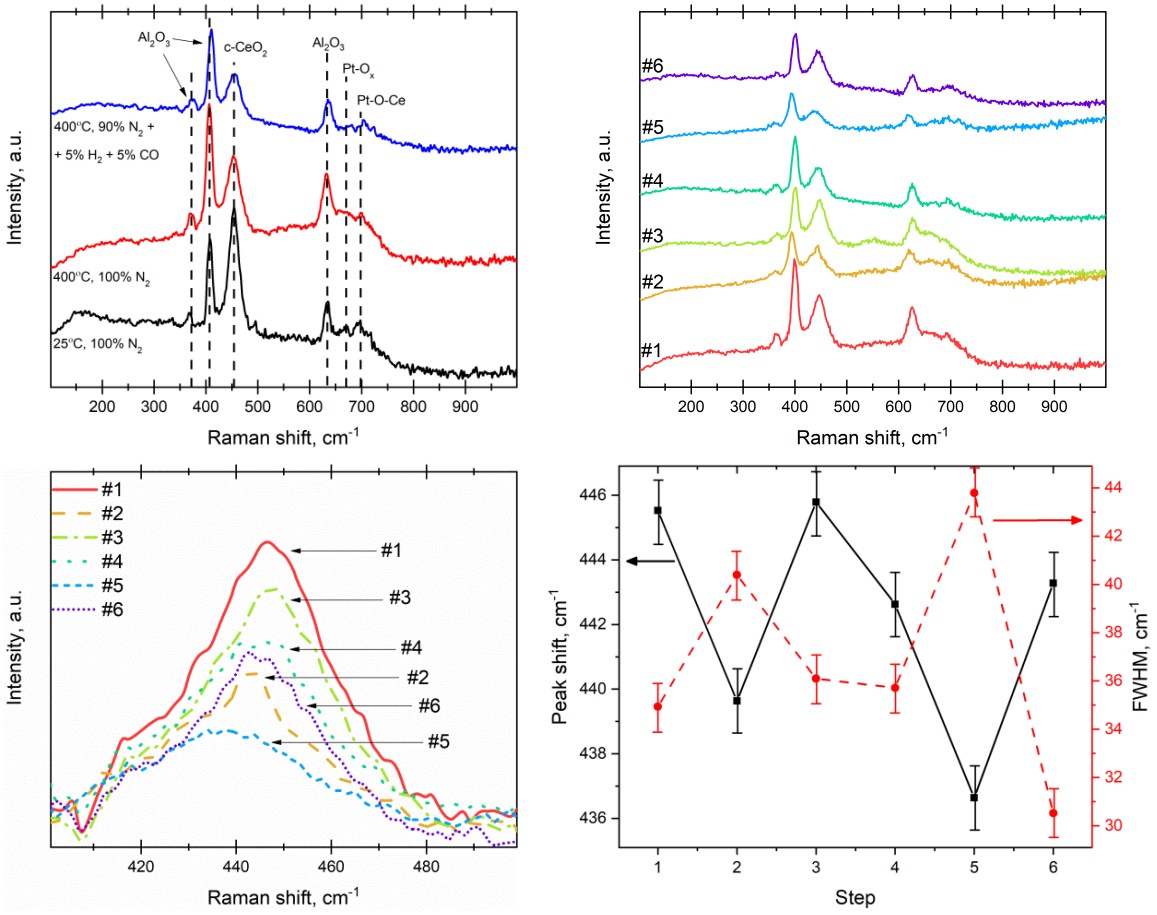

FIG. 3. Raman spectra obtained *in-situ* from Pt/CZ catalyst as a function of temperature and gas conditions (a). Raman spectra obtained according to the sequence of measurement steps (b). A dedicated line of symmetrical oscillations in O–Ce–O depending on gas-temperature conditions (c). Peak shift of $CeO_{2-\delta}$ and its half-width depending on the measurement step (d)

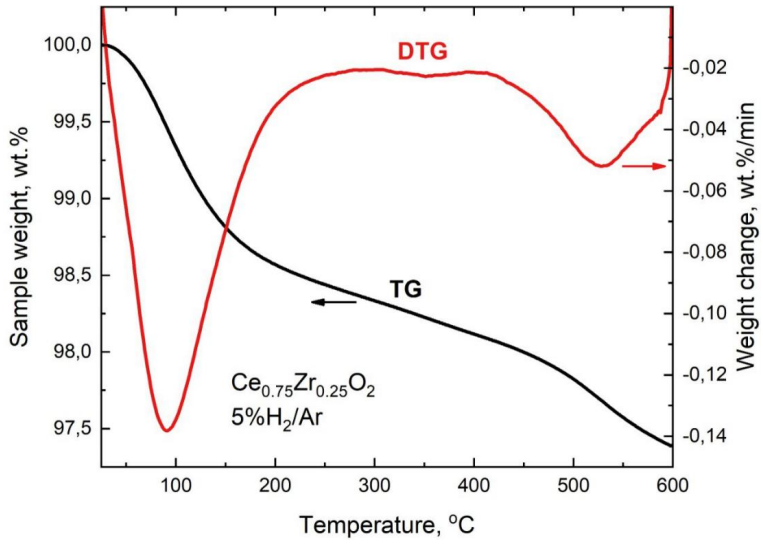

FIG. 4. Results of TG and DTG (differential thermogravimetric analysis) for a catalyst support of the composition $Ce_{0.75}Zr_{0.25}O_2$ in a reducing atmosphere (5 % H_2/Ar)

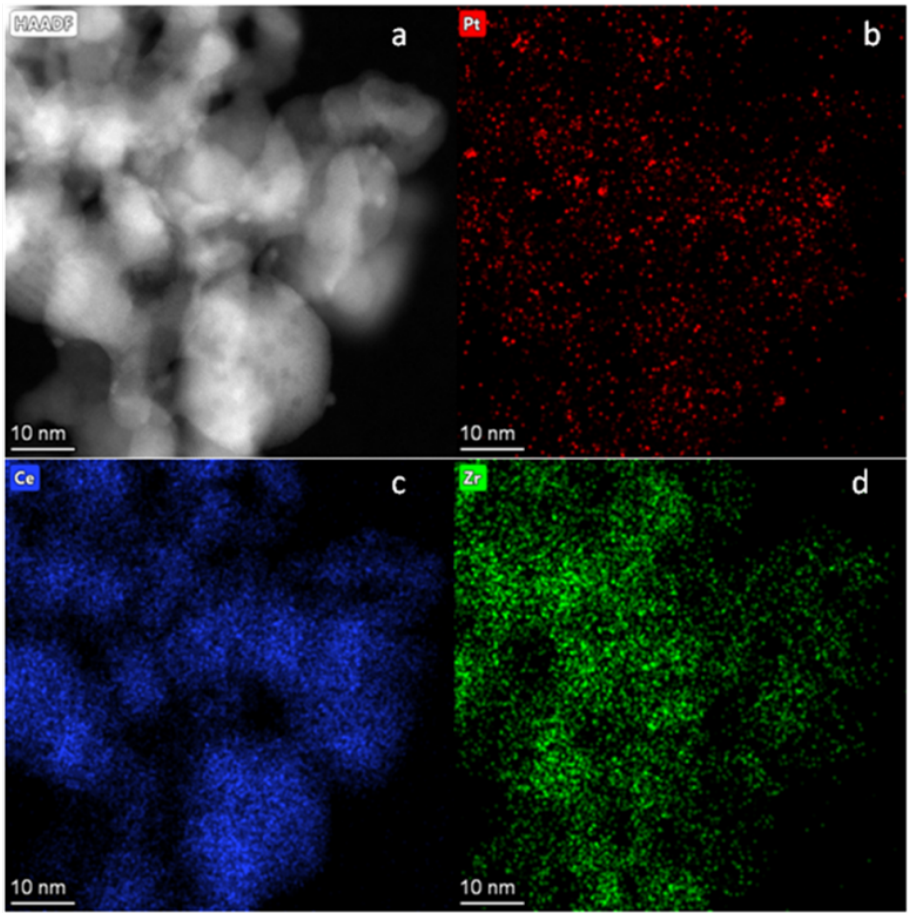

FIG. 5. HAADF-STEM image (a) and corresponding Pt (b), Ce (c) and Zr (d) mapping for as-prepared 1.9 wt. % Pt/CZ catalyst

4. Conclusions

The Pt/CeO_2–ZrO_2 catalyst demonstrated high catalytic activity in partial oxidation of DMM and DME and was also studied by Raman spectroscopy. Catalyst studies showed that H_2 and CO concentrations at working temperature of 700 °C are close to 35 and 25 vol. % respectively for both DMM and DME partial oxidation reactions. Conversion rates are in turn close to 100 % at this temperature. Thermogravimetric analysis and Raman spectra indicate that the catalyst has high mobility of lattice oxygen. It was shown that both during heating and transition from the inert atmosphere to reducing conditions oxygen escapes from the crystal lattice of the samples. This leads to the formation of oxygen vacancies and, consequently, to an increase in the proportion of Ce^{3+} relative to Ce^{4+}. Returning to the initial external conditions (temperature, inert atmosphere) leads to the reverse process: oxygen (in trace amounts because of inevitable leaks) occupies free vacancies while the concentration of Ce^{4+} returns to the initial values. Thus, during PO reactions oxygen enters the catalytic reaction zone not only from the reaction mixture but also directly from the catalyst support.

Such a "breathing" structure of the catalyst support allows efficient transport of oxygen from the lattice to the catalyst surface, namely to the Pt nanoparticles. It is important to note that there is a possibility of thermal cycling of these catalysts during operation without changing their crystalline properties. Thus, Pt/CZ systems are of particular interest as highly efficient catalysts for syngas production from various hydrocarbons feedstock's for SOFC feeding.

References

[1] Su X., et al. Thermodynamic analysis of fuel composition and effects of different dimethyl ether processing technologies on cell efficiency. *Fuel Proc. Tech.*, 2020, **203**, 106391.

[2] Tu B., et al. Thermodynamic analysis and experimental study of electrode reactions and open circuit voltages for methane-fuelled SOFC. *Int. J. Hydrog. Energy*, 2020, **45** (58), P. 34069–34079.

[3] Hartwell A.R., et al. Effects of Synthesis Gas Concentration, Composition, and Operational Time on Tubular Solid Oxide Fuel Cell Performance. *Sustainability*, 2022, **14** (13), 7983.

[4] Li B., et al. Study on the operating parameters of the 10 kW SOFC-CHP system with syngas. *Int. J. Coal Sci. Technol.*, 2021, **8**, P. 500–509.

[5] Badmaev S.D., et al. Partial Oxidation of Dimethoxymethane to Syngas Over Supported Noble Metal Catalysts. *Top. Catal.*, 2020, **63** (1-2), P. 196–202.

[6] Badmaev S.D., et al. Partial Oxidation of Dimethyl Ether by Air into Synthesis Gas over Pt- and Rh/$Ce_{0.75}Zr_{0.25}O_{2-\delta}$ Catalysts. *Int. J. Hydrog. Energy*, 2021, **46** (72), P. 35877–35885.
[7] Navarro R.M., et al. Hydrogen production reactions from carbon feedstocks: fossil fuels and biomass. *Chem. Rev.*, 2007, **107**, P. 3952–3991.
[8] Chen Y., et al. Partial oxidation of dimethyl ether to H_2/syngas over supported Pt catalyst. *J. Nat. Gas Chem.*, 2008, **17**, P. 75–80.
[9] Shoynkhorova T.B., et al. Highly dispersed Rh-, Pt-, Ru/$Ce_{0.75}Zr_{0.25}O_{2-\delta}$ catalysts prepared by sorption-hydrolytic deposition for diesel fuel reforming to syngas. *Appl. Catal. B*, 2018, **237**, P. 237-244.
[10] Chung C.-H., et al. Critical Roles of Surface Oxygen Vacancy in Heterogeneous Catalysis over Ceria-based Materials: A Selected Review. *Chem. Lett.*, 2021, **50** (5), P. 856–865.
[11] Damyanova S., et al. The effect of CeO_2 on the surface and catalytic properties of Pt/CeO_2–ZrO_2 catalysts for methane dry reforming. *Appl. Catal. B*, 2009, **89** (1–2), P. 149–159.
[12] Tan W., et al. Highly efficient Pt catalyst on newly designed CeO_2-ZrO_2-Al_2O_3 support for catalytic removal of pollutants from vehicle exhaust. *Chem. Eng. J.*, 2021, **426**, 131855.
[13] Korableva G.M., et al. Application of High-temperature Raman Spectroscopy (RS) for Studies of Electrochemical Processes in Solid Oxide Fuel Cells (SOFCs) and Functional Properties of their Components. *ECS Trans.*, 2021, **103** (1), P. 1301–1317.
[14] Eliseeva G.M., et al. In-situ Raman spectroscopy studies of oxygen spillover at solid oxide fuel cell anodes. *Chem. Prob.*, 2020, **1** (18), P. 9–19.
[15] Weber W.H., et al. Raman study of CeO_2: Second-order scattering, lattice dynamics, and particle-size effects. *Phys. Rev. B*, 1993, **48**, P. 178–185.
[16] Schilling C., et al. Raman Spectra of Polycrystalline CeO_2: A Density Functional Theory Study. *J. Phys. Chem. C*, 2017, **121**, P. 20834–20849.
[17] Brogan M.S., et al. Raman spectroscopic study of the Pt-CeO_2 interaction in the Pt/Al_2O_3-CeO_2 catalyst. *J. Chem. Soc. Faraday Trans.*, 1994, **90**, P. 1461–1466.
[18] Lin W., et al. Probing Metal-Support Interactions under Oxidizing and Reducing Conditions: In Situ Raman and Infrared Spectroscopic and Scanning Transmission Electron Microscopic-X-ray Energy-Dispersive Spectroscopic Investigation of Supported Platinum Catalysts. *J. Phys. Chem. C*, 2008, **112**, P. 5942–5951.
[19] Berezhinsky L.I., et al. Investigation of Al-ZERODUR interface by Raman and secondary ion mass-spectroscopy. *Semicond. Phys. Quantum Electron. Optoelectron.*, 2005, **8** (2), P. 37–40. http://dx.doi.org/10.15407/spqeo8.02.037.
[20] Lee J., et al. How Pt Interacts with CeO_2 under the Reducing and Oxidizing Environments at Elevated Temperature: The Origin of Improved Thermal Stability of Pt/CeO_2 Compared to CeO_2. *J. Phys. Chem. C*, 2016, **120** (45), P. 25870–25879.
[21] Schmitt R., et al. A review of defect structure and chemistry in ceria and its solid solutions. *Chem. Soc. Rev.*, 2020, **49**, P. 554–592.

Submitted 20 August 2024; revised 15 April 2025; accepted 2 July 2025

Information about the authors:

Galina M. Korableva – Osipyan Institute of Solid State Physics RAS, Acad. Osipyana, 2, Chernogolovka, Moscow District, 142432, Russia; ORCID 0000-0002-6353-5753; eliseevagm@issp.ac.ru

Dmitrii A. Agarkov – Osipyan Institute of Solid State Physics RAS, Acad. Osipyana, 2, Chernogolovka, Moscow District, 142432, Russia; Moscow Institute of Physics and Technology, Institutskiy per., 9, Dolgoprudny, Moscow District, 141701, Russia; ORCID 0000-0001-9650-6951; agarkov@issp.ac.ru

Sukhe D. Badmaev – Boreskov Institute of Catalysis SB RAS, Lavrentiev Ave., 5, Novosibirsk, 630090, Russia; ORCID 0000-0001-6351-8219; sukhe@catalysis.ru

Denis S. Katrich – Osipyan Institute of Solid State Physics RAS, Acad. Osipyana, 2, Chernogolovka, Moscow District, 142432, Russia; ORCID 0009-0002-9316-8488; katrich.ds@phystech.edu

Alexandr V. Samoilov – Osipyan Institute of Solid State Physics RAS, Acad. Osipyana, 2, Chernogolovka, Moscow District, 142432, Russia; ORCID 0000-0001-8579-6340; samoilov@issp.ac.ru

Pavel V. Snytnikov – Boreskov Institute of Catalysis SB RAS, Lavrentiev Ave., 5, Novosibirsk, 630090, Russia; ORCID 0000-0002-5057-3187; pvsnyt@catalysis.ru

Ilya I. Tartakovskii – Osipyan Institute of Solid State Physics RAS, Acad. Osipyana, 2, Chernogolovka, Moscow District, 142432, Russia; tartakov@issp.ac.ru

Sergey I. Bredikhin – Osipyan Institute of Solid State Physics RAS, Acad. Osipyana, 2, Chernogolovka, Moscow District, 142432, Russia; ORCID 0000-0002-8616-2531; bredikh@issp.ac.ru

Conflict of interest: the authors declare no conflict of interest.